

CHANDRA OBSERVATIONS OF GALACTIC SUPERNOVA REMNANT VELA JR.: A NEW SAMPLE OF THIN FILAMENTS EMITTING SYNCHROTRON X-RAYS

AYA BAMBA,¹ RYO YAMAZAKI,² AND JUNKO S. HIRAGA³

Received 2005 February 3; accepted 2005 June 14

ABSTRACT

The Galactic supernova remnant (SNR) Vela Jr. (RX J0852.0–4622, G266.6-1.2) shows sharp filamentary structures on its northwestern edge in the hard X-ray band. The filaments are very smooth and located on the extreme outside edge of the remnant. We measured the averaged scale width of the filaments (w_u and w_d) with excellent spatial resolution with *Chandra*, and they are on the order of the size of the point-spread function of *Chandra* on the upstream side and $49''.5$ ($36''.0$ – $88''.8$) on the downstream side. The spectra of the filaments are very hard and have no linelike structure; they were well reproduced with an absorbed power-law model with $\Gamma = 2.67$ (2.55–2.77) or a SRCUT model with $\nu_{\text{roll}} = 4.3$ (3.4 – 5.3) $\times 10^{16}$ Hz under the assumption of $p = 0.3$. These results imply that the hard X-rays are synchrotron radiation emitted by accelerated electrons, as mentioned previously. Using a correlation between the function $\mathcal{B} \equiv \nu_{\text{roll}}/w_d^2$ and the SNR age, we estimated the distance and the age of Vela Jr.: the estimated distance and age are 0.33 (0.26–0.50) kpc and 660 (420–1400) yr, respectively. These results are consistent with previous reports, implying that the \mathcal{B} -age relation may be a useful tool for estimating the distance and the age of synchrotron X-ray-emitting SNRs.

Subject headings: acceleration of particles — ISM: individual (G266.6-1.2, RX J0852.0–4622) — supernova remnants — X-rays: ISM

1. INTRODUCTION

Supernova remnants (SNRs) play crucial roles in the heating and chemical evolution of galaxies. Their shocks are also famous as cosmic-ray accelerators. Koyama et al. (1995) discovered synchrotron X-rays from shells of SN 1006, which is the first observational result indicating that SNRs accelerate electrons up to \sim TeV. By now, several SNRs have been identified as synchrotron X-ray emitters (e.g., RX J1713.7–3946, Koyama et al. 1997; Slane et al. 1999; RCW 86, Bamba et al. 2000; Borkowski et al. 2001; Rho et al. 2002; Cas A, Vink & Laming 2003; see also Bamba et al. 2005; Bamba 2004).

The most plausible acceleration mechanism is diffusive shock acceleration (DSA; e.g., Bell 1978; Drury 1983; Blandford & Eichler 1987; Jones & Ellison 1991; Malkov & Drury 2001), which can accelerate charged particles on the shock into a power-law distribution, similar to the observed spectrum of cosmic rays on the Earth. However, since there is still little observational information and theoretical understanding, there are many unresolved problems, such as the injection efficiency, the maximum energy of accelerated particles, the configurations of the magnetic field, and so on. The magnetic field amplification is also pointed out as a remarkable process (Bell & Lucek 2001; Lucek & Bell 2000). Recently, it has been found that nonthermal X-rays from the shells of historical SNRs concentrate on very narrow filamentary regions (Bamba et al. 2003b, 2005). Together with the roll-off frequency (ν_{roll}) of synchrotron X-rays (Reynolds 1998; Reynolds & Keohane 1999), Bamba et al. (2005) found that an empirical function, $\mathcal{B} \equiv \nu_{\text{roll}}/w_d^2$, decreases with the age of an

SNR (\mathcal{B} -age relation). The relation may reflect the time evolution of the magnetic field around the shock front (Bamba et al. 2005). However, the \mathcal{B} -age relation still has many uncertainties because of poor statistics. Clearly, other new samples with synchrotron X-ray filaments are desired.

Vela Jr. (RX J0852.0–4622, G266.6-1.2) is one of the most curious Galactic SNRs, with a large radius of about $60'$ (Green 2004). It was discovered by *ROSAT* (*Röntgensatellit*; Aschenbach 1998), and it is well known that the COMPTEL (Compton Telescope) team reported a possible detection of the 1.157 MeV γ -ray line emitted by ^{44}Ti (Iyudin et al. 1998). This fact strongly indicates that Vela Jr. is a nearby and very young SNR because the half-life of ^{44}Ti is only about 60 yr; however, there remains some doubt about the detection (Schönfelder et al. 2000). Tsunemi et al. (2000) reported the presence of the Ca K line, suggesting that there is plenty of Ca produced from ^{44}Ti . On the other hand, Slane et al. (2001) reported that the 1σ upper limit of the Sc K line is $4.4 \times 10^{-6} \text{ cm}^{-2} \text{ s}^{-1}$. Recently, Iyudin et al. (2005) reported a possible detection of Ti and Sc K emission lines with *XMM-Newton*. For the 78.4 keV line emission from ^{44}Ti , von Kienlin et al. (2005) obtained an upper limit of $1.1 \times 10^{-4} \text{ cm}^{-2} \text{ s}^{-1}$ with *INTEGRAL* (*International Gamma-Ray Astrophysics Laboratory*) SPI. The presence of a central source has also been suggested (Aschenbach 1998), which was confirmed with *Chandra* (Pavlov et al. 2001). The spectrum of the source, CXOU J085201.4–461753, together with the absence of any optical counterpart (Mereghetti et al. 2002), reminds us of a neutron star. These observational reports might indicate that the progenitor is a core-collapse supernova (SN).

The other fact that makes this SNR famous is the existence of nonthermal X-rays from the rims (Slane et al. 2001), which implies that the rims of Vela Jr. are cosmic-ray accelerators like SN 1006 (Koyama et al. 1995) and other SNRs with synchrotron X-rays (e.g., Bamba 2004 and references therein). Recently, TeV γ -rays with energies greater than 500 GeV have also been detected at the 6σ level from the northwestern rim of the SNR with CANGAROO-II (Collaboration of Australia and Nippon for a

¹ RIKEN (Institute of Physical and Chemical Research) 2-1, Hirosawa, Wako, Saitama 351-0198, Japan; bamba@crab.riken.jp.

² Department of Earth and Space Science, Graduate School of Science, Osaka University, Toyonaka, Osaka 560-0043, Japan; ryo@vega.ess.sci.osaka-u.ac.jp.

³ Department of High Energy Astrophysics, Institute of Space and Astronautical Science (ISAS), Japan Aerospace Exploration Agency (JAXA), 3-1-1 Yoshinodai, Sagami-hara, Kanagawa 229-8510, Japan; jhiraga@astro.isas.jaxa.jp.

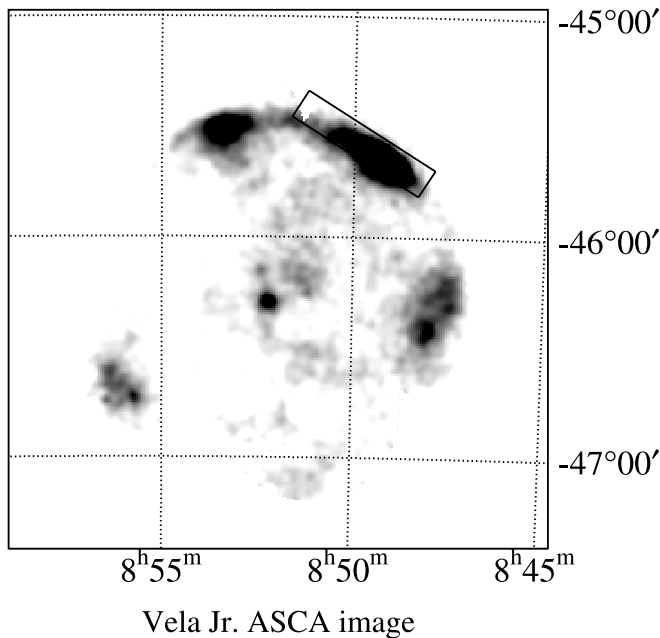


FIG. 1.—*ASCA* GIS image of Vela Jr. in the 0.7–10.0 keV band (Tsunemi et al. 2000). The gray scale is logarithmic, and coordinates are J2000.0. The solid rectangle shows the field of view of the *Chandra* ACIS-S array.

Gamma Ray Observatory in the Outback; Katagiri et al. 2005) and HESS (High Energy Stereoscope System; Aharonian et al. 2005). These γ -rays are produced by accelerated electrons and/or protons with energies $>\sim 1$ TeV.

Despite being such an interesting source, the precise age of the remnant is still unknown. There are some spikes in nitrate concentration measured in an Antarctic ice core, which might be regarded as signals of SNe (Burgess & Zuber 2000). One of them is not yet identified with any known historical SN. If the spike is really associated with the progenitor of Vela Jr., the SN may have occurred around AD 1320 and the age of the remnant is about 680 yr. However, there are many uncertainties; hence, further studies are necessary. In addition, an unclear issue is the distance to the remnant, which would bring us a great deal of information, such as the total luminosity of the ^{44}Ti emission line, the average expansion velocity, and so on. It might also be able to resolve the current debate about whether or not Vela (at a distance of 250 pc; Cha et al. 1999) and Vela Jr. interact with each other. Iyudin et al. (1998) estimated the distance to be ~ 200 pc with an assumption that the age is 680 yr, as mentioned above, while Slane et al. (2001) suggested that the distance is 1–2 kpc based on the relatively large absorption column. Although Moriguchi et al. (2001) observed the molecular distribution using ^{12}CO ($J = 1-0$) emission with NANTEN, they could not determine the precise distance because the remnant is located near the tangential point of a Galactic arm. The upper limit of the distance that they estimated is ~ 1 kpc.

In this paper, using the *Chandra* data for the first time, we report on the analysis of hard X-ray filaments associated with Vela Jr. and discuss the acceleration mechanism at the shock of the SNR, its age, and the distance to the SNR. This paper is organized as follows. We summarize the details of the observation of Vela Jr. with *Chandra* in § 2. Section 3 describes the results of the observations. We discuss the ^{44}Sc emission line reported by Iyudin et al. (2005) in § 4, the origin of nonthermal X-rays in § 5, the interaction between the SNR and molecular clouds in § 6, and on the origin of TeV γ -rays in § 7. In § 8, we discuss the distance

TABLE 1
OBSERVATION LOG

ObsID	R.A.	Decl.	Date	Exposure (ks)
3846.....	08 49 09.3	−45 37 42.4	2003 Jan 5	39
4414.....	08 49 09.3	−45 37 42.3	2003 Jan 6	35

NOTE.—Units of right ascension are hours, minutes, and seconds, and units of declination are degrees, arcminutes, and arcseconds.

and the age of the SNR using the correlation between the function \mathcal{B} and the SNR age.

2. OBSERVATIONS

We used archival *Chandra* ACIS data of the northwestern (NW) rim of Vela Jr. (ObsIDs 3846 and 4414). Figure 1 shows the *ASCA* (*Advanced Satellite for Cosmology and Astrophysics*) GIS image (Tsunemi et al. 2000) with the field of view of the *Chandra* observations. The satellite and the instrument are described by Weisskopf et al. (2002) and Garmire et al. (2000), respectively. Data acquisition from ACIS was done in the Timed-Exposure Faint mode. The data reduction and analysis were performed using the *Chandra* Interactive Analysis of Observations (CIAO) software, version 3.0.2. Using the Level 2 processed events provided by the pipeline processing at the *Chandra* X-Ray Center, we selected *ASCA* grades 0, 2, 3, 4, and 6 as the X-ray events. The “streak” events on the CCD chip S4 were removed using the algorithm *destreak*⁴ in CIAO. In order to make the statistics better, we improved the astrometry of the data following the CIAO data analysis threads and combined these data. The exposure times of the observations are 39 ks (ObsID 3846) and 35 ks (ObsID 4414). Table 1 summarizes these observations. Hereafter, all results are from the combined data unless stated otherwise.

3. RESULTS

Figure 2 shows images of the NW rim in the 0.5–2.0 keV (Fig. 2a) and 2.0–10.0 keV (Fig. 2b) bands, binned with a $4''$ scale. Neither subtraction of background photons, smoothing process, nor correction of the exposure time were performed. The difference of background level among the chips is caused by that of the CCD chips (back-illuminated and front-illuminated). These images look alike and clearly show very straight filamentary structures on the outer edge of the rim. Two filaments can be recognized well, especially in Figure 2a. Iyudin et al. (2005) suggest that the inner filament may be the reverse shock emission. However, we have no clue to distinguish whether it indicates the reverse shock or an apparently overlaid forward shock via the projection effect. The filaments are very similar to those in SN 1006 (Long et al. 2003; Bamba et al. 2003b), indicating that they may be efficient accelerators of electrons like the SN 1006 filaments. Then we performed an analysis in the same way as our previous one for SN 1006 (Bamba et al. 2003b).

For the first step, we made a spectrum from the whole emitting region of this rim. Since the rim is covered by two CCD chips (chips 6 and 7), source spectra were made separately from each chip. Background photons were accumulated from outer regions of the rim. All the spectra extend up to >2 keV, indicating that the hard X-ray emission is nonthermal. There is some linelike feature below 2 keV, which probably comes from thermal emission of Vela and/or Vela Jr., as already mentioned (Slane et al. 2001).

⁴ See <http://asc.harvard.edu/ciao2.3/ahelp/destreak.html>.

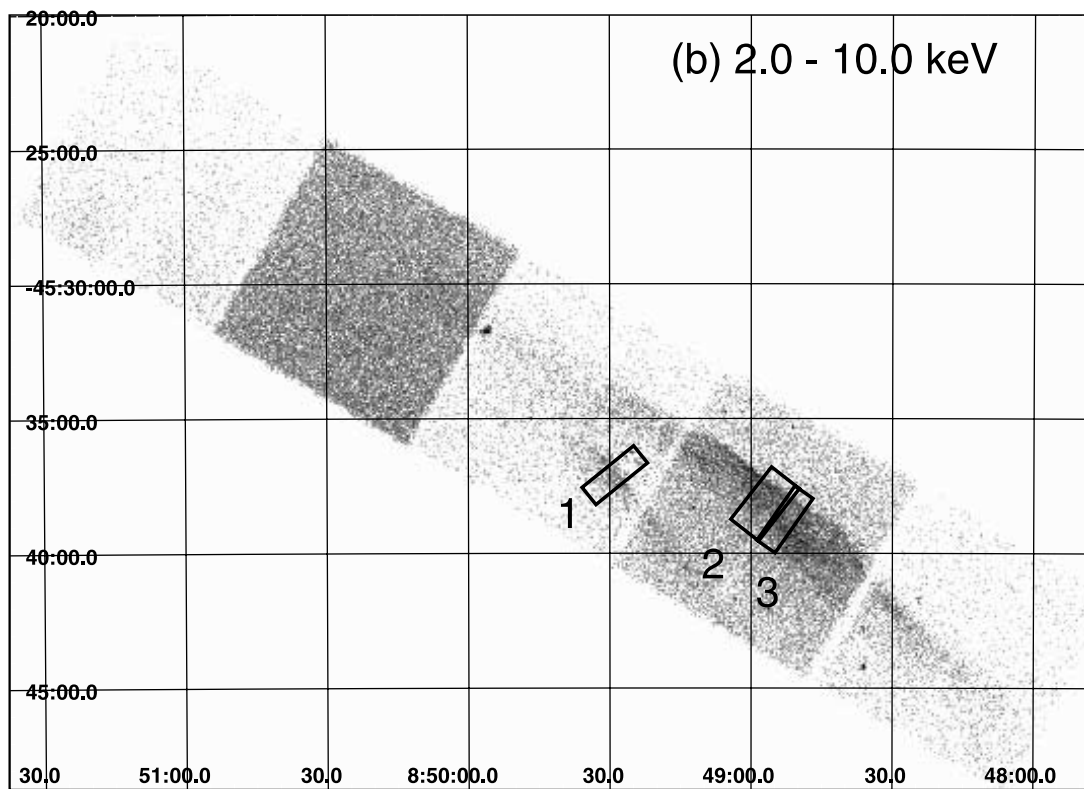
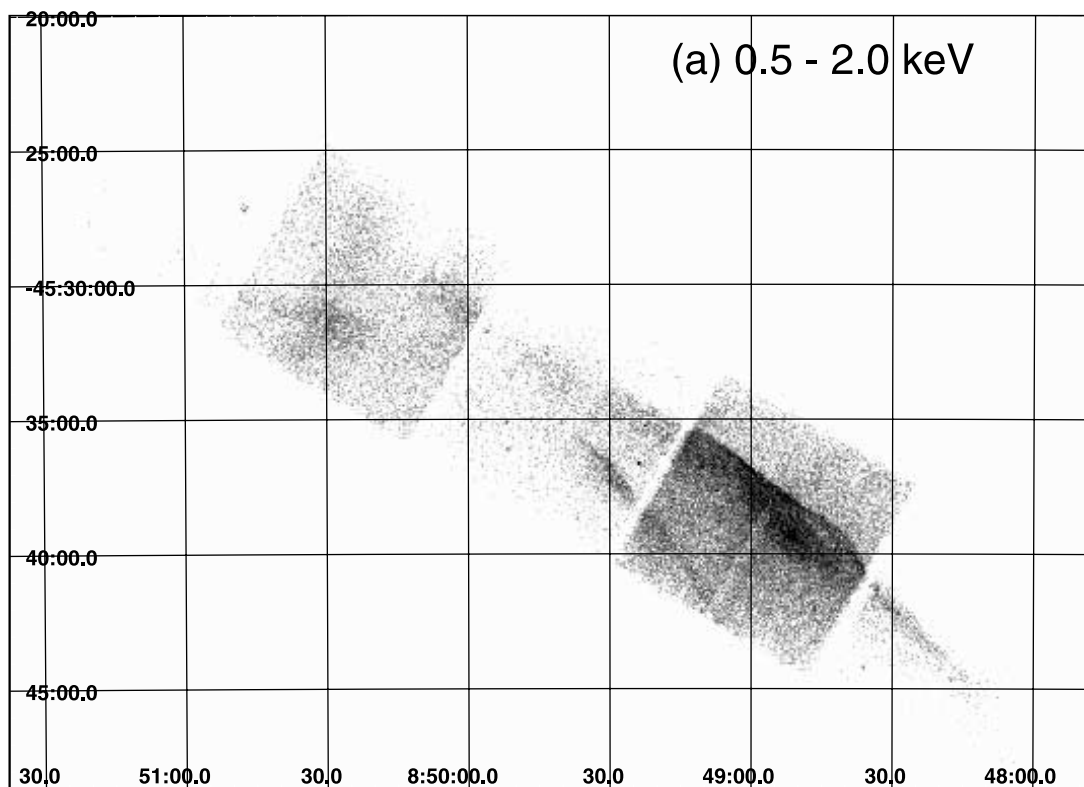


FIG. 2.—*Chandra* images of the NW rim of Vela Jr. in (a) the 0.5–2.0 keV band and (b) the 2.0–10.0 keV band. Gray scales are logarithmic and coordinates are J2000.0, binned with a $4''$ scale. Regions to make profiles are shown in (b) with solid rectangles.

TABLE 2
BEST-FIT PARAMETERS OF THE SPECTRUM OF THE NW RIM

Parameters	Best-Fit Value ^a
Γ	2.67 (2.52–2.84)
N_{H} (10^{21} H cm ⁻²) ^b	6.1 (2.4–9.9)
Flux ^c (10^{-12} ergs cm ⁻² s ⁻¹)	6.2 (5.9–6.5)
χ^2/dof	114.4/135

^a Parentheses indicate single-parameter 90% confidence regions.

^b Calculated using the cross sections by Morrison & McCammon (1983) with the solar abundances (Anders & Grevesse 1989).

^c In the 2.0–10.0 keV band.

Since our data do not have sufficient statistics to examine the properties of thermal plasma, we ignored that component. In Hiraga et al. (2005), detailed analysis for the thermal plasma is done with the *XMM-Newton* deep observation. We fitted the spectra with an absorbed power-law model only with photons above 2 keV, in order to avoid the contamination of thermal photons. The absorption column was subsequently calculated using the cross sections by Morrison & McCammon (1983) with the solar abundances (Anders & Grevesse 1989). The best-fit parameters are shown in Table 2.

The best-fit values of the photon index and absorption column are consistent with those of the nonthermal component in previous results (Slane et al. 2001; Iyudin et al. 2005; Hiraga et al. 2005), indicating that almost all photons above 2 keV are of nonthermal origin. Thus, we regard all the photons above 2 keV as nonthermal in the following. As shown in Figure 2b, three filaments were selected (filaments 1–3) in order to study their spatial and spectral characteristics, which are straight and free from other structures, in the same way as in the analysis of the SN 1006 case (Bamba et al. 2003b). Since all the filaments are located within $4'$ from the aim point (see Table 1), the size of the point-spread function (PSF) is about $0''.5$. Although we can see the filaments more clearly in the soft X-ray band in Figure 2, Bamba et al. (2003b) showed that the contamination of thermal photons makes filaments broader. Therefore, we conducted the spatial analysis only with photons above 2 keV. Figure 3 shows spatial profiles of the filaments in the 2.0–10.0 keV (nonthermal) band binned to a resolution of $1''$. We can see profiles with clear decays on the downstream sides and sharp edges on the upstream sides in all profiles. Filaments 2 and 3 are double peaked, as suggested by Iyudin et al. (2005). To estimate the scale width of these filaments on the upstream (w_u) and downstream (w_d) sides, we fitted them with an exponential function as a simple and empirical fitting model for the apparent profiles, which is the same as used

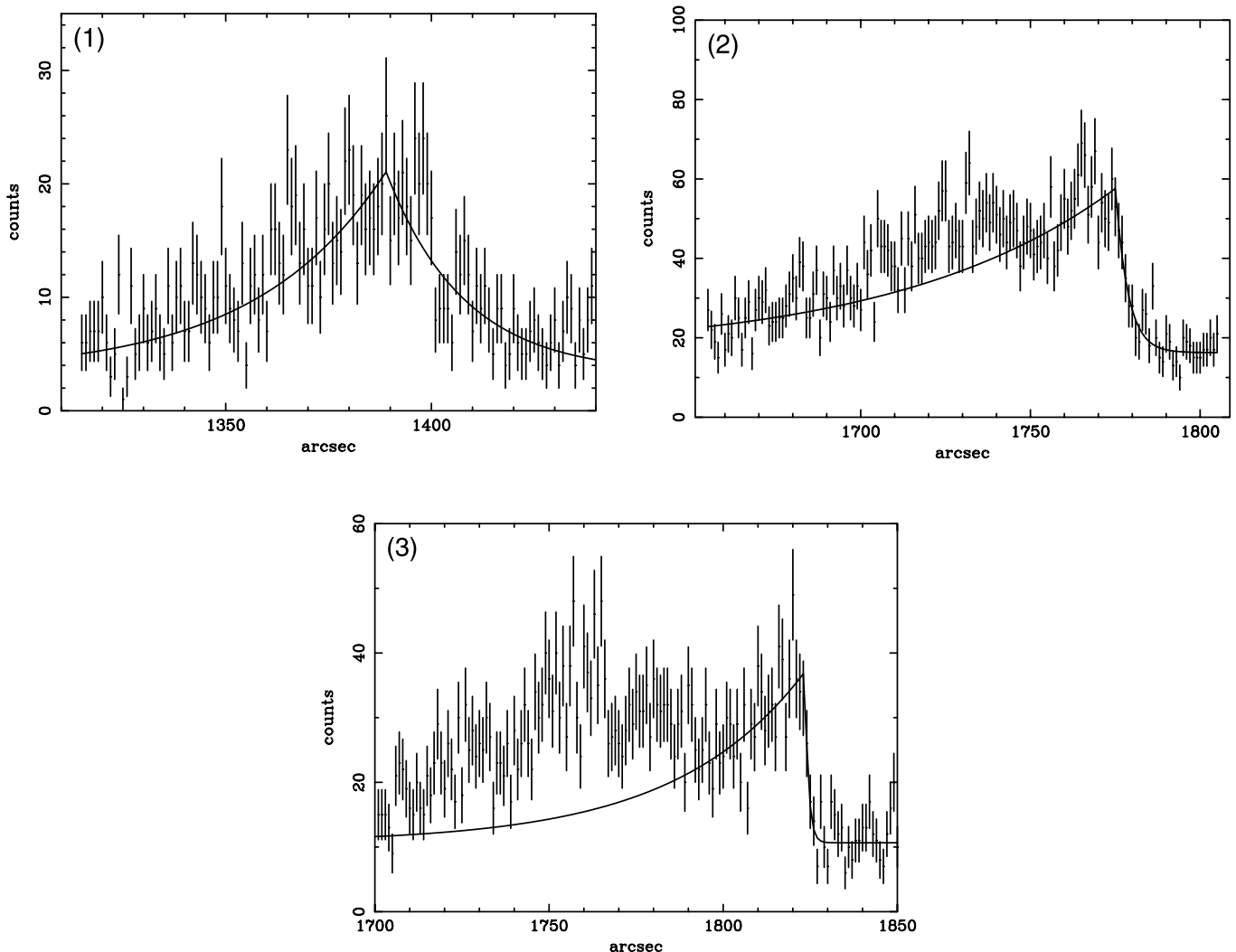


FIG. 3.—Profiles of the filaments in the 2.0–10.0 keV band, binned with a $1''$ scale. The best-fit models are shown with solid lines. In each panel, the shock runs from left to right. For filaments 2 and 3, each fitting was carried out only around the outer peak in order to avoid the contamination from the inner peak.

TABLE 3
BEST-FIT PARAMETERS OF THE PROFILES OF THE FILAMENTS

Number	A (counts arcsec ⁻¹)	w_u (arcsec)	w_d (arcsec)	Reduced χ^2 (χ^2/dof)
1.....	17.8 (15.8–19.9)	19.0 (12.1–31.4)	31.8 (23.7–47.1)	143.4/121
2.....	41.4 (36.5–47.4)	3.68 (2.69–5.75)	65.0 (38.2–144.6)	56/51
3.....	26.4 (22.4–30.7)	^a	37.1 (26.5–60.2)	58/54
Mean ^b	49.5 (34.8–98.3)	...

NOTE.—Parentheses indicate single-parameter 90% confidence regions.

^a Fixed to 1".

^b Flux-weighted mean value.

in the previous analyses of SN 1006 (Bamba et al. 2003b) and other historical SNRs (Bamba et al. 2005). Background photons were not subtracted and treated as a spatially independent component. For filament 3, w_u could not be determined due to the lack of statistics, so it was frozen at the PSF size (0".5). For each filament, the fitting region was limited around the outermost peak in order to avoid the influence of the inner structure. The model reproduced the data well. The best-fit models and parameters are shown in Figure 3 and Table 3, respectively.

For the next step, we made spectra of the filaments. The background regions were selected from the downstream sides of the filaments, where there was no other structure. The spectra were very hard and were fitted with an absorbed power-law model again. The absorption column was fixed to 6.1×10^{21} cm⁻² in order to make the statistics better, which is the best-fit value for the total region (Table 2) and consistent with previous results. The index of the power-law component is similar to those of nonthermal shells in other SNRs (SN 1006, Bamba et al. 2003b; RX J1713.7–3946, Koyama et al. 1997; Slane et al. 1999), which is considered to be synchrotron emission. Therefore, we concluded that the nonthermal emission in the Vela Jr. shell is synchrotron, and we applied the SRCUT model, which is one of the models representing the synchrotron emission from electrons of a power-law distribution with exponential roll-off in a homogeneous magnetic field (Reynolds 1998; Reynolds & Keohane 1999). The spectral index at 1 GHz was fixed to 0.3 according to a report by Combi et al. (1999). Since the value $p = 0.3$ is rather smaller than those of ordinary SNRs (~ 0.5), we also tested the model under the assumption of $p = 0.5$. All models can reproduce the data with similar values of reduced χ^2 as shown in Table 4.

4. COMMENTS ON ⁴⁴Sc FLUORESCENT LINE

Iyudin et al. (2005) reported a significant emission line at 4.45 ± 0.05 keV from the NW rim of Vela Jr. with *XMM-Newton*.

We checked the spectrum of each filament, as well as the averaged one, so as to investigate the presence of some linelike feature. As a result, we found that the spectrum of filament 1 has an excess around 4 keV as shown in Figure 4, while the spectrum averaged for the whole rim does not show that line feature. Since one can see the excess in the data of both observations, it may be a real line. Then the power law plus a narrow line model were applied and accepted, although the reduced χ^2 does not improve significantly ($\chi^2/\text{dof} = 69.5/79$; see also Table 4). The center energy is 4.1 ± 0.2 keV, which is slightly lower than the averaged one by Iyudin et al. (2005) but consistent with the *ASCA* result (Tsunemi et al. 2000). The total flux, $7.3^{+5.1}_{-4.5} \times 10^{-7}$ photons cm⁻² s⁻¹, is about 10% of that derived by Iyudin et al. (2005) and Tsunemi et al. (2000) and consistent with the upper limit by Slane et al. (2001). The difference of the intensity may be because of our smaller region for the spectral analysis than those by other authors. Moreover, the center energy and significance depend on the choice of the background region and the model of the continuum component. The lack of statistics prevents us from a reliable conclusion. Detailed analysis with excellent statistics and spectral resolution are encouraged.

5. ORIGIN OF THE FILAMENTS

We found that the scale width of the filaments in Vela Jr. is much smaller than its radius. Filament 3 has a small w_u on the order of the *Chandra* PSF size (0".5), indicating that w_u may be similar to or smaller than the PSF size. Although the other filaments have w_u that are significantly larger than the PSF size, it may be caused by the projection effect or other structures, such as the second peak and/or other filaments. Therefore, we concluded that the scale width on the upstream side is similar to or smaller than the PSF size. On the other hand, the value of w_d is much larger than the PSF size. These results are similar to other cases of nonthermal filaments in young SNRs (Bamba et al. 2005). The

TABLE 4
BEST-FIT PARAMETERS OF THE SPECTRA OF THE FILAMENTS

NUMBER	POWER LAW			SRCUT ($p = 0.3$)			SRCUT ($p = 0.5$)		
	Γ	Flux ^a	χ^2/dof	ν_{roll}^b	$\Sigma_{1\text{GHz}}^c$	χ^2/dof	ν_{roll}^b	$\Sigma_{1\text{GHz}}^c$	χ^2/dof
1.....	2.87 (2.71–3.06)	0.74 (0.63–0.85)	76.2/81	2.7 (1.8–3.8)	4.4 (2.8–3.8)	79.2/81	3.7 (2.6–5.8)	148 (95–230)	76.1/81
2.....	2.59 (2.44–2.74)	1.8 (1.6–2.1)	137.3/118	5.3 (3.6–7.3)	1.2 (1.1–1.3)	141.3/118	8.2 (5.5–12.8)	120 (113–127)	141.3/118
3.....	2.45 (2.23–2.68)	0.76 (0.61–0.92)	56.2/44	7.4 (4.1–13.2)	0.93 (0.84–1.01)	57.7/44	11.6 (6.4–25.7)	32 (28–36)	57.4/44
Total.....	2.67 (2.57–2.77)	3.2 (2.9–3.6)	276.8/245	4.3 (3.4–5.3)	8.8 (8.1–9.5)	286.6/245	6.6 (5.0–8.7)	282 (262–301)	284.9/245

NOTES.—The absorption column was fixed to 6.1×10^{21} H cm⁻² according to Table 2. Parentheses indicate single-parameter 90% confidence regions.

^a Absorption-corrected flux in the 2.0–10.0 keV band in units of 10^{-13} ergs cm⁻² s⁻¹.

^b Roll-off frequency in units of 10^{16} Hz.

^c Flux density at 1 GHz in units of 10^{-4} Jy.

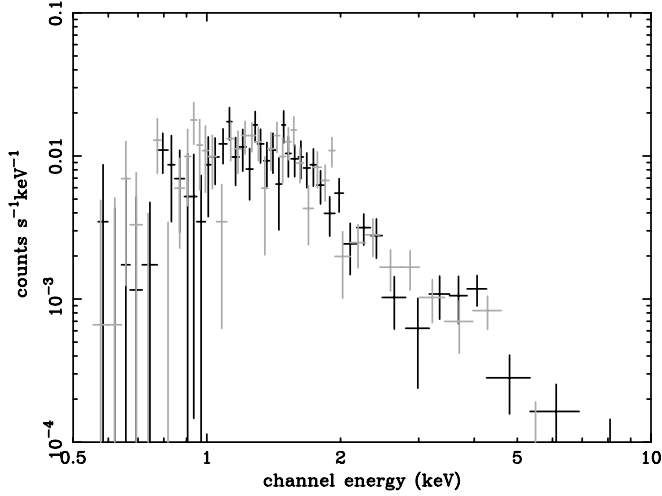


FIG. 4.—Spectra of filament 1 showing data for ObsIDs 3846 (black) and 4414 (gray).

power-law index is similar to the results with previous observations (Slane et al. 2001; Hiraga et al. 2005). These thin filaments with hard X-rays remind us of the nonthermal X-rays from filaments in young SNRs. Wideband spectra of most of these SNRs show that the nonthermal X-rays are synchrotron radiation from highly accelerated electrons. Therefore, we consider the filaments to emit X-rays via synchrotron radiation. In order to confirm our conclusion, we need more information in the radio continuum band to make the wideband spectrum of synchrotron emission.

6. INTERACTION WITH MOLECULAR CLOUDS?

The filaments in Vela Jr. are rather straight, and their lengths are comparable to the radius of the SNR, which are similar to those in SN 1006 (Bamba et al. 2003b) and Tycho (Hwang et al. 2002) and are unlike the clumpy filaments in Cas A (Vink & Laming 2003), RCW 86 (Rho et al. 2002), and RX J1713.7–3946 (Uchiyama et al. 2003; Lazendic et al. 2004; Cassam-Chenai et al. 2004). The former samples are located in tenuous interstellar space, whereas for the two SNRs in the latter cases, there are some reports about the interaction between shocks and molecular clouds (RCW 86: Y. Moriguchi et al. 2001, private communication; RX J1713.7–3946: Fukui et al. 2003). Interactions with molecular clouds may distort beautiful filaments via turbulence and so on. There are molecular clouds around Vela Jr. (Moriguchi et al. 2001). However, it is not clear whether the shocks are interacting with them or not because there is no observation with excited molecular cloud lines [CO (2 → 1) and so on]. The straight filaments may indicate that there is no interaction between the shock and the molecular cloud in this region. Further observations with excited molecular lines are needed.

7. ORIGIN OF TeV γ -RAYS

Recently, two instruments have independently detected TeV γ -rays significantly (Katagiri et al. 2005; Aharonian et al. 2005). The reported differential fluxes are consistent with each other, but the photon indexes are slightly different. In this section, we examine the origin of the TeV γ -rays, considering the preferable values of the maximum energy of electrons (E_{\max}) and the downstream magnetic field (B_d ; Yamazaki et al. 2004). Bamba et al. (2005) suggested that the width of the filament on the downstream side (w_d) and the roll-off frequency of synchrotron emission (ν_{roll}) reflect the value of E_{\max} and B_d , so we can use these

two observational values for the study of E_{\max} and B_d . Hereafter, we adopt flux-averaged mean values, such as

$$w_d = 49''5 = 0.24^{+0.19}_{-0.07} \left(\frac{D}{1 \text{ kpc}} \right) \text{ pc}, \quad (1)$$

$$\nu_{\text{roll}} = 6.6^{+2.1}_{-1.6} \times 10^{16} \text{ Hz}, \quad (2)$$

where D is the distance to Vela Jr. Considering the projection effect, w_d can be written as

$$w_d = \alpha r^{-1} u_s t_{\text{loss}},$$

$$t_{\text{loss}} = 1.25 \times 10^3 \text{ yr} \left(\frac{E_{\max}}{100 \text{ TeV}} \right)^{-1} \left(\frac{B_d}{10 \mu\text{G}} \right)^{-2},$$

where α , r , u_s , and t_{loss} are correction factors of the projection effect, the compression ratio, the shock velocity, and the synchrotron loss timescale, respectively (Bamba et al. 2005; Yamazaki et al. 2004). Although α is an unknown parameter depending on the shape of profiles and the curvature radius, it becomes $\sim 1-10$ as far as the width of filaments is negligible to the SNR radii (Berezhko & Völk 2004). Then the above equations lead to

$$\left(\frac{E_{\max}}{100 \text{ TeV}} \right)^{-1} \left(\frac{B_d}{10 \mu\text{G}} \right)^{-2} = 6.3^{+5.0}_{-1.8} \times 10^{-2} \alpha^{-1} r$$

$$\times \left(\frac{u_s}{3000 \text{ km s}^{-1}} \right)^{-1} \frac{D}{1 \text{ kpc}}. \quad (3)$$

On the other hand, the roll-off frequency ν_{roll} is represented as (Reynolds & Keohane 1999; Reynolds 1998)⁵

$$\nu_{\text{roll}} = (1.6 \times 10^{18}) \text{ Hz} \left(\frac{E_{\max}}{100 \text{ TeV}} \right)^2 \frac{B_d}{10 \mu\text{G}}. \quad (4)$$

In the following, we adopt typical values $\alpha = 5$ and $r = 4$. Then using equations (3) and (4), we derived

$$E_{\max} = (4.1^{+0.9}_{-0.9} \text{ TeV}) \left(\frac{D}{1 \text{ kpc}} \right)^{1/3}$$

$$\times \left(\frac{\alpha}{5} \right)^{-1/3} \left(\frac{r}{4} \right)^{1/3}, \quad (5)$$

$$B_d = (2.2^{+0.2}_{-0.2} \times 10^2 \mu\text{G}) \left(\frac{u_s}{3000 \text{ km s}^{-1}} \right)^{2/3}$$

$$\times \left(\frac{D}{1 \text{ kpc}} \right)^{-2/3} \left(\frac{\alpha}{5} \right)^{2/3} \left(\frac{r}{4} \right)^{-2/3}. \quad (6)$$

Katagiri et al. (2005) examined whether the TeV γ -rays arise from the inverse Compton emission via accelerated electrons or π^0 decay caused by accelerated protons. The former requires a very high size ratio of X-ray and TeV γ -ray emission regions ($V_{\text{TeV}}/V_{\text{X-ray}} \sim 10^5$) and a strong magnetic field of $B_d \sim 1.6 \text{ mG}$. Then we obtain the shock velocity with equation (6) as

$$u_s \sim (6 \times 10^8 \text{ cm s}^{-1}) \frac{D}{100 \text{ pc}} \left(\frac{\alpha}{5} \right)^{-1} \frac{r}{4}, \quad (7)$$

⁵ See <http://heasarc.gsfc.nasa.gov/docs/xanadu/xspec> for the erratum of coefficients.

so that the small distance, $D \lesssim 100$ pc (the very small physical radius and the very young age, in other words) may be required, which is somewhat doubtful. This result is consistent with the discussion in Aharonian et al. (2005). On the other hand, the π^0 -decay model, which requires the interaction of the SNR and molecular clouds, can naturally explain the multiband spectrum (Katagiri et al. 2005). However, there might be some discrepancy between the observed straight filaments as discussed in § 6.

8. ESTIMATION OF THE AGE AND THE DISTANCE

More definitive arguments on the distance (D) are possible, and at this time, the age of the SNR (t_{age}) can be also discussed simultaneously. As a tool of the estimation, the \mathcal{B} -age relation (Bamba et al. 2005) is used, where

$$\mathcal{B} \equiv \frac{\nu_{\text{roll}}}{w_d^2} = C t_{\text{age}}^\alpha, \quad (8)$$

$$C = 2.6_{-1.4}^{+1.2} \times 10^{27} \text{ Hz pc}^{-2}, \quad (9)$$

$$\alpha = -2.96_{-0.06}^{+0.11}. \quad (10)$$

Let θ_R ($\equiv R_s/D$) and θ_d ($\equiv w_d/D$) be the angular radius of the SNR and the observed angular scale width of synchrotron X-ray filaments on the downstream sides, respectively. Here R_s is the radius of the SNR in units of parsecs. From the equation defining \mathcal{B} , we obtain

$$D = (0.65 \text{ kpc}) \frac{10''}{\theta_d} \left(\frac{\nu_{\text{roll}}}{10^{17} \text{ Hz}} \right)^{1/2} \left[\frac{\mathcal{B}(t_{\text{age}})}{10^{20} \text{ Hz pc}^{-2}} \right]^{-1/2}. \quad (11)$$

The thin solid and dashed lines in Figure 5 represent the relation between the age and the distance using equations (11), (1), and (2).

On the other hand, $D = R_s/\theta_R$ is rewritten as

$$D = (0.34 \text{ kpc}) \frac{10' R_s(t_{\text{age}})}{\theta_R \text{ 1 pc}}, \quad (12)$$

$$R_s(t_{\text{age}}) = \begin{cases} (1.1 \text{ pc}) \left(\frac{E_{51}}{M_{\text{ej}} \rho_0} t_{\text{age}}^4 \right)^{1/7}, & t < t_{\text{ST}}, \\ (1.2 \text{ pc}) \left(\frac{E_{51}}{\rho_0} \right)^{1/5} \left(t_{\text{age}} - 0.22 E_{51}^{-1/2} M_{\text{ej}}^{5/6} \rho_0^{-1/3} \right)^{2/5}, & t > t_{\text{ST}}. \end{cases} \quad (13)$$

The function $R_s(t_{\text{age}})$ is given by Truelove & McKee (1999, see eqs. [1] and [2] and Tables 6 and 7), which studies the shock dynamics of SNRs, where E_{51} , M_{ej} , ρ_0 , and t_{ST} are the explosion energy in units of 10^{51} ergs, the ejecta mass in units of M_\odot , the ambient density in units of g cm^{-3} , and the timescale that SNRs enter the Sedov-Taylor phase (in which the shock begins to decelerate due to the interstellar medium), respectively (Truelove & McKee 1999). For simplicity, we consider the case of the constant interstellar medium, n_0 ,

$$n_0 \equiv \frac{\rho_0}{\mu_{\text{H}}}, \quad (14)$$

where μ_{H} is the mean mass per hydrogen nucleus, $1.4 \times 1.67 \times 10^{-24}$ g. In the following, we choose the kinetic energy of the ejecta, the ejecta mass, and n_0 to be 10^{51} ergs, $1.4 M_\odot$, and

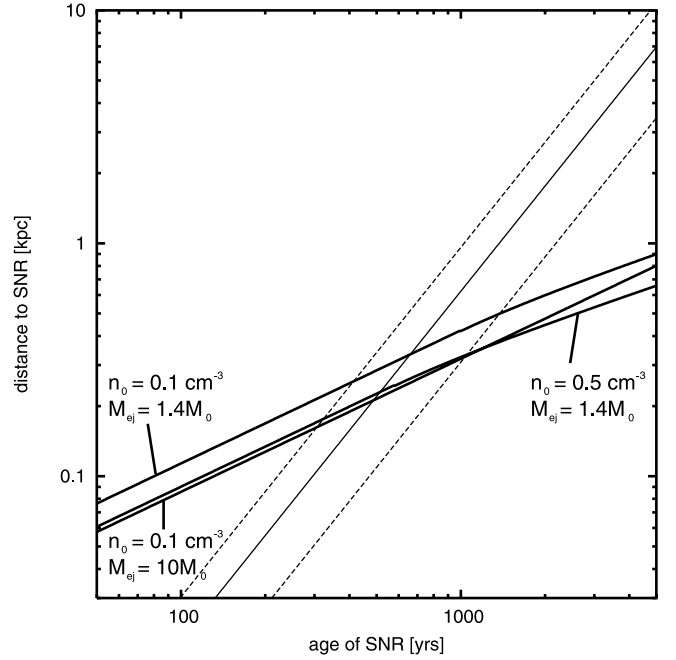


FIG. 5.—Relations between the age and the distance derived from the evolution of SNRs and from the function \mathcal{B} . The thick, solid, and dashed lines are the relations from the SNR model, and best-fit one from the function \mathcal{B} and their allowed regions, respectively.

0.1 cm^{-3} , respectively. Solving these equations, one can estimate both D and t_{age} .

Figure 5 represents the relation between the age and the distance. We derived the allowed range of the parameters to be

$$t_{\text{age}} = 660 (420\text{--}1400) \text{ yr}, \quad (15)$$

$$D = 0.33 (0.26\text{--}0.50) \text{ kpc}. \quad (16)$$

When we vary the ambient number density to $n_0 = 0.5 \text{ cm}^{-3}$ or the ejecta mass to $M_{\text{ej}} = 10 M_\odot$, the result remains basically unchanged, as can be seen in Figure 5.

Although the allowed regions are too wide to derive any conclusions, we may be able to say that Vela Jr. is a nearby and relatively young SNR. The results are consistent with previous reports, which may imply that this is an indirect confirmation of the \mathcal{B} -age relation (Bamba et al. 2005), and our distance/age indicator may become a useful tool in the future. Furthermore, the derived distance is significantly larger than that of the Vela SNR (250 pc; Cha et al. 1999), so there may be no interaction between these two SNRs.

The most common distance indicator for SNRs is an application of the relation between the surface brightnesses at 1 GHz and the diameters of SNRs (Σ - D relation; Case & Bhattacharya 1998); however, the relation still has large uncertainties. Recent X-ray surveys recognize a new type of SNRs, which are dim in the radio band and bright in the hard X-ray band, such as RX J1713.7–3946 (Koyama et al. 1997), G28.6-0.1 (Bamba et al. 2001; Ueno et al. 2003), and so on (e.g., Combi et al. 2005; Yamaguchi et al. 2004). The number of such SNRs may be more than ~ 20 (Bamba et al. 2003a). They must be significant accelerators of cosmic rays because most of them emit synchrotron X-rays. Unfortunately, they are dim in the radio bands, so the Σ - D relation cannot be directly applied. Our method may also be a useful tool for estimating both D and t_{age} of such synchrotron X-ray-emitting SNRs.

Again let us consider E_{\max} and B_d using equations (5) and (6). Assuming that $D \sim 300$ pc, that is, the most preferable value of our distance indicator, we obtain $E_{\max} \sim 3$ TeV and $B_d \sim 5 \times 10^2 \mu\text{G}$. Although the uncertainty is very large, our result may indicate that the magnetic field is highly amplified.

These results do not include the uncertainty of the model of SNR dynamics and the function \mathcal{B} . When these uncertainties are considered, the allowed regions for t_{age} and D become larger. It is the uncertainty of \mathcal{B} 's normalization that makes the error regions the widest, accounting for $\sim 50\%$. In order to improve this method for determining t_{age} and D , more samples are needed to make the uncertainty of \mathcal{B} smaller.

9. SUMMARY

We have conducted systematic spectral and spatial analysis of filamentary structures in the Vela Jr. NW rim for the first time. A summary of our results is as follows:

1. We found that nonthermal X-rays from the Vela Jr. NW rim are concentrated on very thin filamentary structures. The average scale width on the upstream side is similar to or smaller than the

PSF size of *Chandra*, whereas that on the downstream side is $49''5$ ($36''0$ – $88''8$).

2. The spectra of the filaments are hard and have no linelike structure, which is well reproduced with an absorbed power-law model of $\Gamma = 2.67$ (2.55–2.77) or a SRCUT model with $\nu_{\text{roll}} = 4.3$ (3.4 – 5.3) $\times 10^{16}$ Hz under the assumption of $p = 0.3$.

3. We tried to estimate the distance (D) and the age (t_{age}) of Vela Jr. using the function \mathcal{B} and estimated that $t_{\text{age}} = 660$ (420–1400) yr and $D = 0.33$ (0.26–0.50) kpc, which is consistent with previous reports. These results may suggest that there is no interaction between the Vela SNR and Vela Jr.

4. Using the estimated D , we derived the most preferable values $E_{\max} \sim 3$ TeV and $B_d \sim 500 \mu\text{G}$. Our result may imply that the magnetic field of the filament is highly amplified.

Our particular thanks are due to the anonymous referee and to K. Makishima, F. Takahara, Y. Mochizuki, Y. Moriguchi, Y. Uchiyama, M. Tsujimoto, J. Vink, and K. Ebisawa for their fruitful discussions and comments. R. Y. and J. S. H. are supported by a JSPS Research Fellowship for Young Scientists.

REFERENCES

- Aharonian, F., et al. 2005, *A&A*, 437, L7
 Anders, E., & Grevesse, N. 1989, *Geochim. Cosmochim. Acta*, 53, 197
 Aschenbach, B. 1998, *Nature*, 396, 141
 Bamba, A. 2004, Ph.D. thesis, Kyoto Univ.
 Bamba, A., Tomida, H., & Koyama, K. 2000, *PASJ*, 52, 1157
 Bamba, A., Ueno, M., Koyama, K., & Yamauchi, S. 2001, *PASJ*, 53, L21
 ———. 2003a, *ApJ*, 589, 253
 Bamba, A., Yamazaki, R., Ueno, M., & Koyama, K. 2003b, *ApJ*, 589, 827
 Bamba, A., Yamazaki, R., Yoshida, T., Terasawa, T., & Koyama, K. 2005, *ApJ*, 621, 793
 Bell, A. R. 1978, *MNRAS*, 182, 443
 Bell, A. R., & Lucek, S. G. 2001, *MNRAS*, 321, 433
 Berezhko, E. G., & Völk, H. J. 2004, *A&A*, 419, L27
 Blandford, R. D., & Eichler, D. 1987, *Phys. Rep.*, 154, 1
 Borkowski, K. J., Rho, J., Reynolds, S. P., & Dyer, K. K. 2001, *ApJ*, 550, 334
 Burgess, C. P., & Zuber, K. 2000, *Astropart. Phys.*, 14, 1
 Case, G. L., & Bhattacharya, D. 1998, *ApJ*, 504, 761
 Cassam-Chenaï, G., Decourchelle, A., Ballet, J., Sauvageot, J.-L., Dubner, G., & Giacani, E. 2004, *A&A*, 427, 199
 Cha, A. N., Sembach, K. R., & Danks, A. C. 1999, *ApJ*, 515, L25
 Combi, J. A., Benaglia, P., Romero, G. E., & Sugizaki, M. 2005, *A&A*, 431, L9
 Combi, J. A., Romero, G. E., & Benaglia, P. 1999, *ApJ*, 519, L177
 Drury, L. O'C. 1983, *Rep. Prog. Phys.*, 46, 973
 Fukui, Y., et al. 2003, *PASJ*, 55, L61
 Garmire, G., Feigelson, E. D., Broos, P., Hillenbrand, L. A., Pravdo, S. H., Townsley, L., & Tsuboi, Y. 2000, *AJ*, 120, 1426
 Green, D. A. 2004, *A Catalogue of Galactic Supernova Remnants* (ver. 2004 January; Cambridge: Mullard Radio Astron. Obs.), <http://www.mrao.cam.ac.uk/surveys/snrs>
 Hiraga, J. S., Kishishita, T., Bamba, A., Takahashi, T., Aharonian, F., & Uchiyama, Y. 2005, *ApJ*, submitted
 Hwang, U., Decourchelle, A., Holt, S. S., & Petre, R. 2002, *ApJ*, 581, 1101
 Iyudin, A. F., Aschenbach, B., Becker, W., Dennerl, K., & Haberl, F. 2005, *A&A*, 429, 225
 Iyudin, A. F., et al. 1998, *Nature*, 396, 142
 Jones, F. C., & Ellison, D. C. 1991, *Space Sci. Rev.*, 58, 259
 Katagiri, H., et al. 2005, *ApJ*, 619, L163
 Koyama, K., Kinugasa, K., Matsuzaki, K., Nishiuchi, M., Sugizaki, M., Torii, K., Yamauchi, S., & Aschenbach, B. 1997, *PASJ*, 49, L7
 Koyama, K., Petre, R., Gotthelf, E. V., Hwang, U., Matura, M., Ozaki, M., & Holt, S. S. 1995, *Nature*, 378, 255
 Lazendic, J. S., Slane, P. O., Gaensler, B. M., Reynolds, S. P., Plucinsky, P. P., & Hughes, J. P. 2004, *ApJ*, 602, 271
 Long, K. S., Reynolds, S. P., Raymond, J. C., Winkler, P. F., Dyer, K. K., & Petre, R. 2003, *ApJ*, 586, 1162
 Lucek, S. G., & Bell, A. R. 2000, *MNRAS*, 314, 65
 Malkov, E., & Drury, L. O'C. 2001, *Rep. Prog. Phys.*, 64, 429
 Mereghetti, S., Pellizzoni, A., & de Luca, A. 2002, in *ASP Conf. Ser.* 271, *Neutron Stars in Supernova Remnants*, ed. P. O. Slane & B. M. Gaensler (San Francisco: ASP), 289
 Moriguchi, Y., Yamaguchi, N., Onishi, T., Mizuno, A., & Fukui, Y. 2001, *PASJ*, 53, 1025
 Morrison, R., & McCammon, D. 1983, *ApJ*, 270, 119
 Pavlov, G. G., Sanwal, D., Kızıltan, B., & Garmire, G. P. 2001, *ApJ*, 559, L131
 Reynolds, S. P. 1998, *ApJ*, 493, 375
 Reynolds, S. P., & Keohane, J. W. 1999, *ApJ*, 525, 368
 Rho, J., Dyer, K. K., Borkowski, K. J., & Reynolds, S. P. 2002, *ApJ*, 581, 1116
 Schönfelder, V., et al. 2000, in *AIP Conf. Proc.* 510, *Fifth Compton Symp.*, ed. M. L. McConnell & J. M. Ryan (New York: AIP), 54
 Slane, P., Gaensler, B. M., Dame, T. M., Hughes, J. P., Plucinsky, P. P., & Green, A. 1999, *ApJ*, 525, 357
 Slane, P., Hughes, J. P., Edgar, R. J., Plucinsky, P. P., Miyata, E., Tsunemi, H., & Aschenbach, B. 2001, *ApJ*, 548, 814
 Truelove, J. K., & McKee, C. F. 1999, *ApJS*, 120, 299
 Tsunemi, H., Miyata, E., Aschenbach, B., Hiraga, J., & Akutsu, D. 2000, *PASJ*, 52, 887
 Uchiyama, Y., Aharonian, F. A., & Takahashi, T. 2003, *A&A*, 400, 567
 Ueno, M., Bamba, A., Koyama, K., & Ebisawa, K. 2003, *ApJ*, 588, 338
 Vink, J., & Laming, J. M. 2003, *ApJ*, 584, 758
 von Kienlin, A., et al. 2005, in *Proc. 5th INTEGRAL Science Workshop* (ESA SP-552; Noordwijk: ESA), in press (astro-ph/0407129)
 Weisskopf, M. C., Brinkman, B., Canizares, C., Garmire, G., Murray, S., & Van Speybroeck, L. P. 2002, *PASP*, 114, 1
 Yamaguchi, H., Ueno, M., Koyama, K., Bamba, A., & Yamauchi, S. 2004, *PASJ*, 56, 1059
 Yamazaki, R., Yoshida, T., Terasawa, T., Bamba, A., & Koyama, K. 2004, *A&A*, 416, 595